Monthly Notices
of the
ROYAL ASTRONOMICAL SOCIETY

MNRAS **483,** 5548–5553 (2019)
Advance Access publication 2018 December 22

doi:10.1093/mnras/sty3386

The maximum stellar surface density due to the failure of stellar feedback

Michael Y. Grudić,[1]★ Philip F. Hopkins,[1] Eliot Quataert[2] and Norman Murray[3]†

[1]*TAPIR, Mailcode 350-17, California Institute of Technology, Pasadena, CA 91125, USA*
[2]*Department of Astronomy and Theoretical Astrophysics Center, University of California Berkeley, Berkeley, CA 94720, USA*
[3]*Canadian Institute for Theoretical Astrophysics, 60 St. George Street, University of Toronto, ON M5S 3H8, Canada*

Accepted 2018 December 5. Received 2018 November 15; in original form 2018 April 4

ABSTRACT

A maximum stellar surface density $\Sigma_{\rm max} \sim 3 \times 10^5 {\rm M}_\odot\,{\rm pc}^{-2}$ is observed across all classes of dense stellar systems (e.g. star clusters, galactic nuclei, etc.), spanning ∼8 orders of magnitude in mass. It has been proposed that this characteristic scale is set by some dynamical feedback mechanism preventing collapse beyond a certain surface density. However, simple analytic models and detailed simulations of star formation moderated by feedback from massive stars argue that feedback becomes *less* efficient at higher surface densities (with the star formation efficiency increasing as $\sim\Sigma/\Sigma_{\rm crit}$). We therefore propose an alternative model wherein stellar feedback becomes ineffective at moderating star formation above some $\Sigma_{\rm crit}$, so the supply of star-forming gas is rapidly converted to stars before the system can contract to higher surface density. We show that such a model – with $\Sigma_{\rm crit}$ taken directly from the theory – naturally predicts the observed $\Sigma_{\rm max}$. We find $\Sigma_{\rm max} \sim 100\Sigma_{\rm crit}$ because the gas consumption time is longer than the global free-fall time even when feedback is ineffective. Moreover, the predicted $\Sigma_{\rm max}$ is robust to spatial scale and metallicity, and is preserved even if multiple episodes of star formation/gas inflow occur. In this context, the observed $\Sigma_{\rm max}$ directly tells us where feedback fails.

Key words: galaxies: active – galaxies: evolution – galaxies: formation – galaxies: star clusters: general – galaxies: star formation – cosmology: theory.

1 INTRODUCTION

Hopkins et al. (2010, hereafter Paper I) showed that the central surface densities of essentially all dense stellar systems exhibit the same apparent upper limit $\Sigma_{\rm max} \sim 3 \times 10^5 {\rm M}_\odot\,{\rm pc}^{-2}$. This includes globular clusters (GCs), super-star clusters (SSCs), dwarf and late-type galaxy nuclear star clusters (NSCs), young massive clusters (YMCs), ultra-compact dwarfs (UCDs), compact ellipticals (cEs), galactic bulges, nearby and high-redshift early-type/elliptical galaxies, even nuclear stellar discs around Sgr A∗ and the Andromeda nuclear black hole. These span mass scales of 10^4–$10^{12}\,{\rm M}_\odot$, spatial sizes $0.1 - 10^4$ pc, three-dimensional densities $1 - 10^5\,{\rm M}_\odot\,{\rm pc}^{-3}$ (free-fall times ∼10^4–10^7 yr), *N*-body relaxation times ∼10^6–10^{17} yr, escape velocities ∼20–600 km s^{-1}, metallicities $Z \sim 0.01$–$5\,{\rm Z}_\odot$, and formation redshifts $z \sim 0$–6, yet agree in $\Sigma_{\rm max}$.

In Fig. 1, we compile more recent observations of dense stellar systems of all classes, and find that this still holds largely true, although some NSCs exceeding the fiducial value of $\Sigma_{\rm max}$ by a factor of a few have since been found. Fig. 2 is adapted from the original compilation of mass profiles of individual objects in Paper I – it shows that even many systems with 'effective' surface densities (measured at $R_{\rm eff}$) have *central* surface densities which approach (but do not appear to exceed) $\Sigma_{\rm max}$, at least where resolved.

Paper I speculated that the universality of $\Sigma_{\rm max}$ might owe to stellar feedback processes.[1] After all, it is widely recognized that feedback plays an important role regulating star formation (SF) in cold, dense molecular clouds (see Kennicutt & Evans 2012, for a review). As gas collapses and forms stars, those stars inject energy and momentum into the interstellar medium via protostellar heating and outflows, photoionization and photoelectric heating from ultraviolet photons, stellar winds, radiation pressure, and supernova explosions. All of these mechanisms may moderate SF, either by contributing to the disruption of molecular clouds (Larson 1981; Murray, Quataert & Thompson 2010; Hopkins, Quataert & Murray 2012; Krumholz et al. 2014; Grudić et al. 2018a) or the large-scale

[1]They also discussed some possible explanations related to e.g. mergers, angular momentum transport processes, or dynamical relaxation, which they showed could *not* explain $\Sigma_{\rm max}$ across the wide range of systems observed (e.g. dynamical relaxation cannot dominate the systems with relaxation times much longer than a Hubble time, and global processes unique to galaxy mergers cannot explain star cluster interiors).

★ E-mail: mgrudich@caltech.edu
† Canada Research Chair in Astrophysics

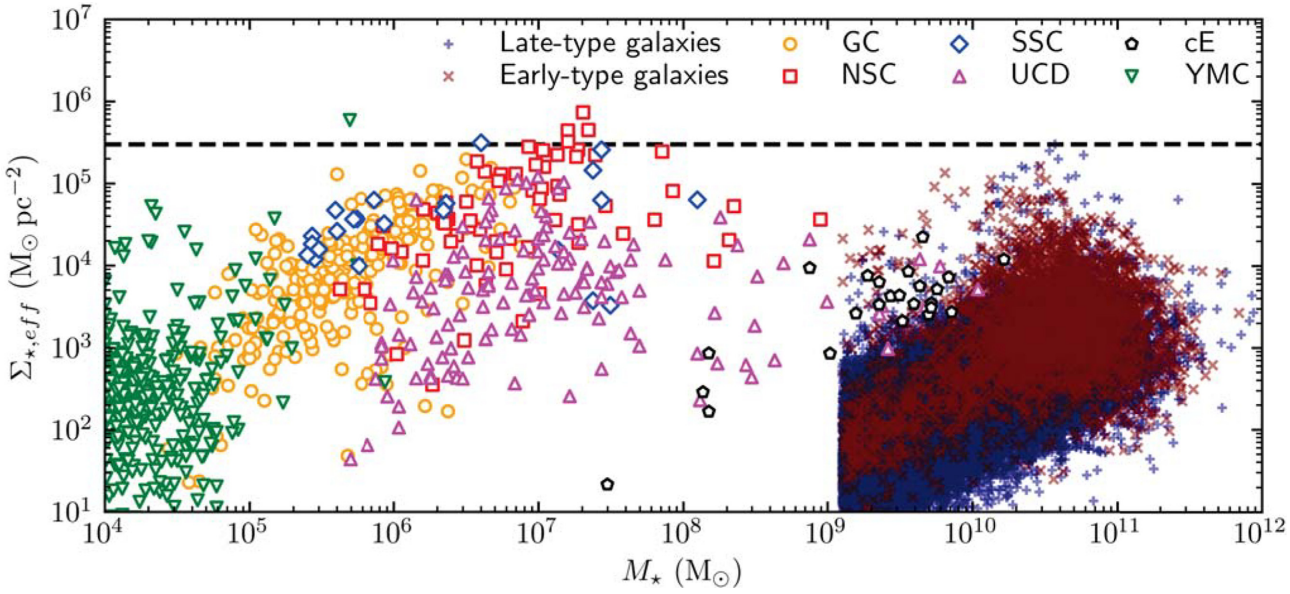

Figure 1. 'Effective' stellar surface density ($\Sigma_{*,\,\rm eff} \equiv M_*/(2\pi R_{\rm eff}^2)$) as a function of stellar mass for various types of stellar systems. Late- and early-type galaxies range from redshifts $z = 0 - 3$ and are taken from van der Wel et al. (2014). GCs, NSCs, UCDs, and cEs are from the compilation of Norris et al. (2014). SSCs are from the populations in M82 (McCrady & Graham 2007), NGC 7252 (Bastian et al. 2013), NGC 34 (Schweizer & Seitzer 2007), and NGC 1316 (Bastian et al. 2006). YMCs are from the Milky Way (Portegies Zwart, McMillan & Gieles 2010) and M83 (Ryon et al. 2015) populations. Dashed: fiducial maximum effective surface density $\Sigma_{\rm max} = 3 \times 10^5 {\rm M}_\odot\,{\rm pc}^{-2}$.

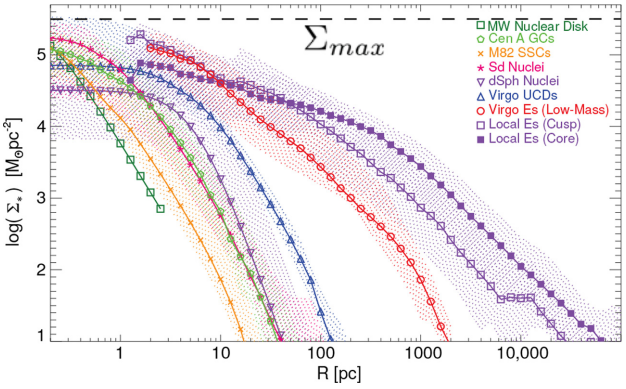

Figure 2. Observed stellar surface density *profiles* $\Sigma_*(r)$ as a function of projected radius, within individual stellar systems – reproduced from fig. 2 of Paper I. Lines show the median $\Sigma_*(r)$ from each sample, and the shaded range shows the $\pm 1\,\sigma$ range in $\Sigma_*(r)$ from all profiles in the sample. Samples are: Milky Way nuclear stellar disc (Lu et al. 2009), Cen A GCs (Rejkuba et al. 2007), M82 SSCs (McCrady & Graham 2007), NSCs in late-type (Sd) galaxy nuclei (Böker et al. 2004), NSCs in dwarf-Spheroidal galaxy nuclei (Geha, Guhathakurta & van der Marel 2002), UCDs in Virgo (Evstigneeva et al. 2007), early-type galaxies in Virgo (separated into low-mass 'dwarf ellipticals' from Kormendy et al. 2009, and massive 'cusp'/steep profile or 'core'/shallow-profile systems from Lauer et al. 2007). Although many of these (e.g. the massive early-type galaxies) have $\Sigma_{*,\,\rm eff}$ (defined at large radii $\gtrsim$kpc) well below $\Sigma_{\rm max}$, all systems appear to approach (and where resolved, saturate around) the fiducial maximum surface density $\Sigma_{\rm max} = 3 \times 10^5 {\rm M}_\odot\,{\rm pc}^{-2}$.

support of galaxies against vertical collapse (Thompson, Quataert & Murray 2005; Ostriker & Shetty 2011; Faucher-Giguère, Quataert & Hopkins 2013; Hopkins et al. 2014; Orr et al. 2018). These mechanisms have various roles on different scales, but stellar feedback is generally the only force strong enough to oppose gravity in dense, star-forming regions, so the characteristic scale of a newly formed stellar system should be determined by the balance point of feedback and gravity.

The specific possibility discussed in Paper I was that multiple scattering of infrared (IR) photons might build up radiation pressure to exceed the Eddington limit for dusty gas. However, the value of $\Sigma_{\rm max}$ predicted according to this argument is inversely proportional to metallicity, so does not explain why $\Sigma_{\rm max}$ is apparently the same in SSCs in metal-rich starbursts (Keto, Ho & Lo 2005; McCrady & Graham 2007) (or super-solar massive elliptical centres) and in metal-poor GCs (or metal-poor high-$z$and low-mass compact galaxies). The argument therein also relied on scalings between IR luminosity and star formation rate (SFR) valid only for continuous-star-forming populations with duration longer than $\sim 10 - 30$ Myr, which exceeds the dynamical times of many of these systems. Finally, Norris et al. (2014) noted that this effect cannot prevent the system from exceeding $\Sigma_{\rm max}$ if SF occurs in multiple episodes.

Since then, various theoretical works have noted the importance of surface density in setting the ratio between the momentum-injection rate from massive stars and the force of self-gravity in a star-forming cloud (Fall, Krumholz & Matzner 2010; Murray et al. 2010; Dekel & Krumholz 2013; Thompson & Krumholz 2016; Raskutti, Ostriker & Skinner 2016; Grudić et al. 2018a). For a cloud with total mass M and stellar mass $M_\star = \varepsilon_{\rm int} M$,

$$\frac{F_{\rm gravity}}{F_{\rm feedback}} \sim \frac{\frac{GM^2}{R^2}}{\epsilon_{\rm int} M \langle \frac{\dot{P}_\star}{M_\star} \rangle} \sim \frac{\Sigma}{\Sigma_{\rm crit}}, \tag{1}$$

where $\langle \frac{\dot{P}_\star}{M_\star} \rangle$ is the specific momentum-injection rate from stellar feedback assuming a simple stellar population with a well-sampled initial mass function (IMF), which is $\sim 10^3 \frac{L_\odot}{M_\odot c}$ for the first 3Myr after SF, and $\Sigma_{\rm crit} \sim \langle \frac{\dot{P}_\star}{M_\star} \rangle / G \approx 3000\,M_\odot\,{\rm pc}^{-2}$ is the characteristic surface density that parametrizes the strength of feedback. If the final SF efficiency (SFE) $\varepsilon_{\rm int}$ is ultimately set by the balance of feedback and gravity, one expects that $\varepsilon_{\rm int} \to 1$ for $\Sigma \gg \Sigma_{\rm crit}$ (Fall et al. 2010). The detailed simulations of Grudić et al. (2018a,

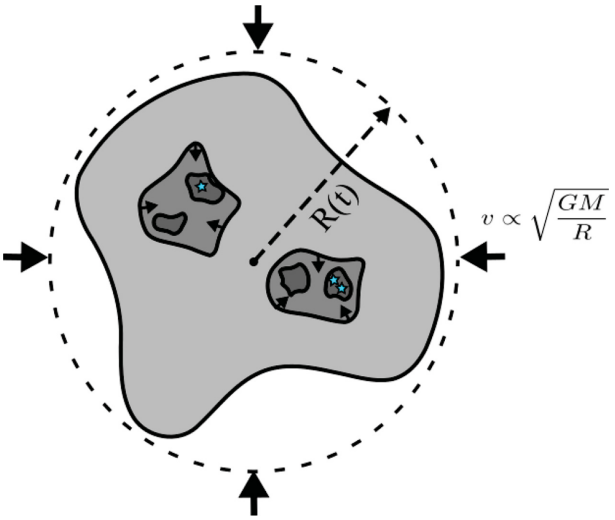

Figure 3. Schematic of our proposed 'best-case' scenario for the formation of a dense stellar system (Section 2.1). A star-forming gas cloud of initial gas mass M is localized within a sphere of radius R. It collapses coherently at the free-fall velocity $v_{\rm ff} = \sqrt{\frac{2GM}{R}}$, while fragmenting locally and forming stars in dense sub-regions. In this 'best case', no dynamical mechanism slows the collapse significantly.

Paper II) showed that this argument is valid across a wide range of metallicities, surface densities and spatial scales, and the final SFE of a molecular cloud is a function mainly of Σ, with weak dependence upon other factors. Paper II also found that the final ratio of stellar mass to initial gas mass, $\varepsilon_{\rm int}$, is proportional to the fraction of gas converted to stars within a free-fall time, $\varepsilon_{\rm ff}$, because a giant molecular cloud tends to form enough stars to destroy itself within a few free-fall times. Thus, Σ should parametrize the per-free-fall efficiency of SF in a manner insensitive to spatial scale and metallicity.

In this paper, we show that if gas contracts globally (for any reason), as it becomes denser (Σ increases), and gravity becomes stronger relative to stellar feedback, gas is converted more and more rapidly into stars (above a characteristic surface density $\Sigma_{\rm crit}$). This exhausts the gas supply, preventing any significant fraction of the inflow from reaching surface densities $> \Sigma_{\rm max}$. We calculate $\Sigma_{\rm max}$ in terms of $\Sigma_{\rm crit}$ and show that the observed $\Sigma_{\rm max} \sim 3 \times 10^5 {\rm M}_\odot\,{\rm pc}^{-2}$ is naturally predicted by the value $\Sigma_{\rm crit} = 3000 {\rm M}_\odot\,{\rm pc}^{-2}$ set by feedback from massive stars (Fall et al. 2010; Grudić et al. 2018a).

2 DERIVATION

2.1 Set-up and assumptions

Consider a discrete SF episode involving a finite collapsing gas mass M, as illustrated in Fig. 3. At a given time, the mass is localized within a radius R, so that its *mean* surface density is:

$$\Sigma = \frac{M}{\pi R^2}. \tag{2}$$

It is forming stars at some SFR, which we can parametrize with the SFE:

$${\rm SFR} \equiv \frac{{\rm d}M_*}{{\rm d}t} = \frac{\epsilon_{\rm ff} M_{\rm gas}}{t_{\rm ff}}, \tag{3}$$

where $\varepsilon_{\rm ff}$ is the (possibly variable) per-free-fall SFE and $t_{\rm ff} = \frac{\pi}{2}\sqrt{\frac{R^3}{2GM}}$ is the free-fall time.

Now, since we are only interested in the *maximum* stellar surface density such a system might reach, we will assume the 'best-case' scenario for forming a dense stellar system. Specifically, assume:

(i) The gas cloud is collapsing at a speed on the order of the escape velocity:

$$\frac{{\rm d}R}{{\rm d}t} = -x_{\rm ff}\sqrt{\frac{2GM}{R}}, \tag{4}$$

where $x_{\rm ff}$ is a constant of order unity.

(ii) There is no support against collapse from large-scale turbulent motions,[2] tidal forces, rotation, shear, magnetic fields, cosmic rays, or the dynamical effects of stellar feedback. We neglect all of these because we are interested in the best-case scenario for producing a dense stellar system according to a give SFE law – any of these may be present, but they will only *slow* collapse, making a lower density system in the end.

This is an idealization, but Kim et al. (2018) did find that bound star clusters do form in a coherent collapse with velocity on the order of the free-fall velocity in cosmological simulations, and stellar feedback does not greatly affect the dynamics until a significant fraction of the gas mass has been converted to stars.

2.2 Star formation efficiency law

We shall assume that $\varepsilon_{\rm ff}$ has some explicit dependence upon Σ, as is motivated by previous work. Accounting for radiation pressure, stellar winds, photoionization heating, and SN explosions, Paper II found

$$\epsilon_{\rm ff} = \epsilon_{\rm ff}(\Sigma) = \left(\frac{1}{\epsilon_{\rm ff}^{\rm max}} + \frac{\Sigma_{\rm crit}}{\Sigma}\right)^{-1}, \tag{5}$$

where $\Sigma_{\rm crit} = 3000 {\rm M}_\odot\,{\rm pc}^{-2}$ is set by the strength of these feedback mechanisms. The dimensionless quantity $\epsilon_{\rm ff}^{\rm max}$ is the maximum per-free-fall SFE attained as $\Sigma \to \infty$. In star-forming clouds supported at a fixed mean surface density, Paper II (see their equation 13 and fig. 5) found that $\epsilon_{\rm ff} \approx 0.34\,\epsilon_{\rm int}$ (where $\varepsilon_{\rm int}$ is the fraction of gas turned into stars over the entire integrated SF history, which of course just saturates at $\epsilon_{\rm int}^{\rm max} = 1$ as $\Sigma \to \infty$). However, this was the median over the entire SF history including initial collapse and eventual blowout. Therefore – in our 'best-case' coherent collapse scenario, we are only interested in the 'peak SFR' event, so $\epsilon_{\rm ff}^{\rm max}$ should be somewhat greater, ~0.5 (see Paper II, fig. 3), and subject to further order-unity corrections due to the different collapse geometry from these simulations. In general, $\epsilon_{\rm ff}^{\rm max}$ should be similar that predicted by turbulent molecular cloud simulations that do not include stellar feedback, which have generally found $\varepsilon_{\rm ff} \sim 0.5{-}1$ in the limit of large turbulent Mach number and realistic turbulent forcing (Federrath & Klessen 2012).

Adding turbulence and magnetic fields in succession, but without feedback initially, Federrath (2015) found average values of $\varepsilon_{\rm ff} \sim 0.1$ and ~0.25 respectively, somewhat lower values than discussed above. These simulations were stopped at an arbitrary integrated SFE of 20 per cent as $\varepsilon_{\rm ff}$, just as $\varepsilon_{\rm ff}$ peaked, which may have reduced the measured average efficiency. These simulations were also at a much lower Mach number, $\mathcal{M} \sim 5$, than the high-efficiency clouds in Paper II, $\mathcal{M} \sim 30$–300, and both analytic theory and simulation

[2]Note that some amount of turbulence must be assumed if stars are forming. We assume that such turbulent eddies are small compared to R, and thus are advected with the large-scale collapse without strongly opposing it.

results find lower values of $\varepsilon_{\rm ff}$ in this $\mathcal{M}$ range when feedback is not present (e.g. Hopkins 2012, fig. 11). Notwithstanding, Federrath (2015) also showed that feedback from protostellar jets could maintain a small $\varepsilon_{\rm ff}$ over several free-fall times. However, we again do not expect this moderation to scale up for clouds of greater $\mathcal{M}$, due to the dimensional scaling of the feedback mechanism. Assuming that outflows coupled a momentum $\langle P_\star/M_\star\rangle$ per stellar mass formed, the value of $\varepsilon_{\rm ff}$ required to support the cloud scales $\propto \sqrt{\frac{GM}{R}}/\langle P_\star/M_\star\rangle \propto \mathcal{M}$, so it is unlikely that protostellar feedback can maintain a low $\varepsilon_{\rm ff}$ in the progenitor clouds of the dense, massive stellar systems considered here (generally with velocity dispersions corresponding to $\mathcal{M} > 30$).

Overall, for the progenitor clouds of the types of system plotted in Fig. 1, we favour values in the range $\varepsilon_{\rm ff,\,max} \sim 0.3$–$0.5$. We acknowledge some amount of uncertainty when generalizing to various geometries and turbulence properties such as solenoidal versus compressive driving.

2.3 Solution

The SFR of the cloud is

$$\frac{{\rm d}M_*}{{\rm d}t} = \epsilon_{\rm ff}\frac{M_{\rm gas}}{t_{\rm ff}} = \frac{M_{\rm gas}}{\left(\epsilon_{\rm ff}^{\rm max}\right)^{-1} + \frac{\Sigma_{\rm crit}}{\Sigma}}\sqrt{\frac{8GM}{\pi^2 R^3}}, \tag{6}$$

where $M_{\rm gas}$ is the gas mass that has not been converted to stars at time t. The differential equation for the gas mass converted to stars when the cloud has radius R follows:

$$\frac{{\rm d}M_{\rm gas}}{{\rm d}R} = -\frac{{\rm d}M_*}{{\rm d}t}\frac{{\rm d}t}{{\rm d}R} = -\frac{2}{\pi x_{\rm ff} R}\frac{M_{\rm gas}}{\left(\epsilon_{\rm ff}^{\rm max}\right)^{-1} + \frac{\pi R^2 \Sigma_{\rm crit}}{M}}. \tag{7}$$

The solution for the fraction of the gas mass surviving to radii $<R$ is

$$\frac{M_{\rm gas}\,(<R)}{M} = \left(1 - \frac{M}{M + \epsilon_{\rm ff}^{\rm max}\pi R^2 \Sigma_{\rm crit}}\right)^{\epsilon_{\rm ff}^{\rm max}/\pi x_{\rm ff}}. \tag{8}$$

Thus, as $R \to 0$, we see that $M_{\rm gas} \to 0$, i.e. the gas is exhausted as the system contracts to surface densities $\Sigma \gg \Sigma_{\rm crit}$. The stellar system formed will subsequently undergo a period of relaxation, but energy conservation requires that the stars remain on orbits with apocentres on the order of the radius R at which they formed .[3] We may thus construct a radial stellar density profile as the superposition of the top-hat mass distributions formed at each radius. The corresponding projected stellar surface density profile is

$$\Sigma_*\,(R) = 2\int_R^\infty \sqrt{R'^2 - R^2}\frac{{\rm d}M_{\rm gas}\,(<R')}{{\rm d}R'}\Big/\left(\frac{4\pi}{3}R'^3\right){\rm d}R', \tag{9}$$

which we plot for various values of $\epsilon_{\rm ff}^{\rm max}$ and $x_{\rm ff}$ in Fig. 4. In general, we find that the characteristic stellar surface densities for plausible values of $\epsilon_{\rm ff}^{\rm max}$ and $x_{\rm ff}$ span the range of surface densities found in dense stellar systems (Figs 1 and 2). Furthermore, if $x_{\rm ff} = 1$ then effective surface densities $\sim 10^5$ M$_\odot$ pc^{-2} are obtained, corresponding to the maximum observed.

It should be noted that the inner surface density profile plotting in Fig. 4 is $\Sigma \propto R^{-2+\frac{2\epsilon_{\rm ff}^{\rm max}}{\pi x_{\rm ff}}}$, which is nearly as steep as R^{-2} for the physically plausible parameters $\epsilon_{\rm ff}^{\rm max} = 0.5$ and $x_{\rm ff} = 1$, ie. the

[3]We have verified with collisionless Monte Carlo simulations that the functional form of equation (8) does closely match the final stellar mass distribution after violent relaxation to virial equilibrium, provided that the initial virial parameter $2E_{\rm kin}/|E_{\rm grav}| \sim 1$.

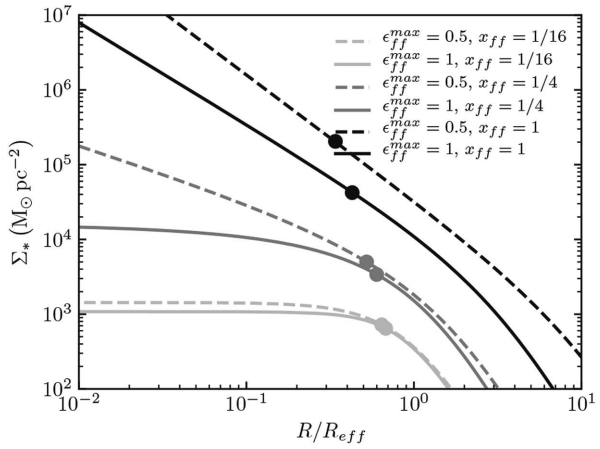

Figure 4. Radial stellar surface density profiles computed from the cloud collapse model described in Section 2.1 for various values of the maximum per-free-fall SFE $\epsilon_{\rm ff}^{\rm max}$ and the rate of collapse relative to free fall $x_{\rm ff}$, with radius in units of the half-mass radius $R_{\rm eff}$. The point on each curve gives the effective stellar surface density $\Sigma_{*,\rm eff} = M_*/\left(2\pi R_{\rm eff}^2\right)$ of the model. The characteristic surface densities obtained over the parameter ranges $\epsilon_{\rm ff}^{\rm max} \sim 0.5 - 1$ and $x_{\rm ff} \sim 0.1$–1 span the range $10^3 - 10^6\ M_\odot\,{\rm pc}^{-2}$ in which most dense stellar systems lie (see Fig. 1). To form a system with $\Sigma_{*,\rm eff} >> 3\times10^5\ M_\odot\,{\rm pc}^{-2}$ would require $\epsilon_{\rm ff}^{\rm max} << 0.5$ or $x_{\rm ff} > >1$, both of which are unphysical.

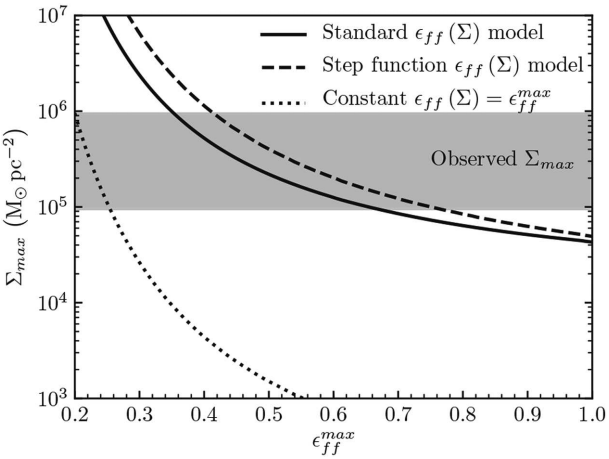

Figure 5. Maximum effective surface density $\Sigma_{\rm max}$ predicted by the model in Section 2.1 as a function of the parameter $\epsilon_{\rm ff}^{\rm max}$ (maximum SFE per-free-fall time, as $\Sigma \to \infty$), assuming $\Sigma_{\rm crit} \approx 3000\ M_\odot\,{\rm pc}^{-2}$. Simulations and analytic theory give $\epsilon_{\rm ff}^{\rm max} \approx 0.5 - 1$ (Hopkins 2012; Federrath & Klessen 2012). Different lines compare different models for how the efficiency $\varepsilon_{\rm ff}$ scales at finite Σ. Solid: our fiducial model (equation 5), where $\varepsilon_{\rm ff}$ scales with $\Sigma/\Sigma_{\rm crit}$ as expected from simple analytic comparison of feedback and gravity (equation 1) or detailed SF simulations (Paper II). Dashed: a model where $\varepsilon_{\rm ff}$ scales as a step function, with $\varepsilon_{\rm ff} = 0.01$ when $\Sigma < \Sigma_{\rm crit}$, and $\varepsilon = \varepsilon_{\rm max}$ when $\Sigma > \Sigma_{\rm crit}$. This gives similar results to the fiducial case, demonstrating that the details of *how* $\varepsilon_{\rm ff}$ scales do not matter here, so long as it rises efficiently above $\sim\Sigma_{\rm crit}$. Dotted: a model with constant $\epsilon_{\rm ff} = \epsilon_{\rm ff}^{\rm max}$, *independent* of surface density Σ. This gives a very steep dependence and can only be reconciled with the observed $\Sigma_{\rm max}$ if we fine-tune $\epsilon_{\rm ff}^{\rm max}$ to a value outside the range predicted by analytic theory and numerical simulations [assuming other mechanisms not considered here cannot reduce it, see Federrath (2015) and discussion in Section 2.2].

profile has nearly constant mass per interval in log R. In such a case, a non-negligible fraction of the mass can be concentrated on scales <0.1pc. Such a high degree of central concentration is not generally found in any type of stellar system, so the inner profiles in this model are an unphysical artefact of the imposed condition of unopposed, spherically-symmetric collapse. This is never realized in nature because even an initially monolithic supersonic collapse is unstable to fragmentation (Guszejnov et al. 2018), and the subsequent violent relaxation of stars produces a much shallower (typically flat) inner density profile (Klessen & Burkert 2001; Bonnell, Bate & Vine 2003; Grudić et al. 2018b). Thus, our free-collapse model lacks the physics necessary to establish a hard limit upon the central stellar surface density,[4] although it should scale in a similar way to the effective surface density when combined with the action of the scale-free physics of gravity and turbulence during SF.

In Fig. 5, we consdier the maximally free-falling case $x_{\rm ff} = 1$ to plot the dependence of $\Sigma_{\rm max}$ on $\epsilon_{\rm ff}^{\rm max}$. We find that if $\Sigma_{\rm crit} = 3000 {\rm M}_\odot\,{\rm pc}^{-2}$ and the plausible range for $\epsilon_{\rm ff}^{\rm max}$ is 0.5−1, the predicted $\Sigma_{\rm max}$ lies within an order of magnitude of the observed $\Sigma_{\rm max} \sim 3\times10^5 {\rm M}_\odot\,{\rm pc}^{-2}$ (Fig. 1). We also present results for two alternate models for $\varepsilon_{\rm ff}(\Sigma)$: a constant value, and a step function equal to 0.01 (e.g. Kennicutt 1998; Krumholz, Dekel & McKee 2012) below $\Sigma_{\rm crit}$ and $\epsilon_{\rm ff}^{\rm max}$ above $\Sigma_{\rm crit}$. First, we note that while our preferred model gives $\Sigma_{\rm max}$ independently of initial cloud surface density, these do not – we therefore take the initial density to be $100 {\rm M}_\odot\,{\rm pc}^{-2}$, typical of local GMCs (Bolatto et al. 2008). Second, we see the '$\varepsilon_{\rm ff}=$ constant' model predicts a $\Sigma_{\rm max}$ that is more sensitive to the chosen $\varepsilon_{\rm ff}$ (and the 'preferred' value, ∼0.2, is small). The step-function model, however, gives very similar results to our default model, so we see that the conclusions are not specific to the *details* of how $\varepsilon_{\rm ff}$ scales, so long as $\varepsilon_{\rm ff}$ is small when $\Sigma < \Sigma_{\rm crit}$ and grows to a value of order unity above $\Sigma \sim \Sigma_{\rm crit}$. Ultimately, the 2 dex separation between $\Sigma_{\rm crit}$ and $\Sigma_{\rm max}$ can be understood as follows: the system forms stars slowly until reaching $\Sigma \sim \Sigma_{\rm crit}$, and only then does significant SF happen, during which global collapse still proceeds. Thus, this system is significantly denser than $\Sigma_{\rm crit}$ at the median SF time.

3 DISCUSSION

We have shown that the observed, apparently universal maximum stellar surface density of dense stellar systems is a natural consequence of feedback-regulated SF physics. Specifically, assuming standard stellar evolution and feedback physics (from e.g. the combination of stellar winds, radiation pressure, SNe, etc.), then as surface densities (Σ) increase, the strength of gravity relative to feedback (assuming some fixed fraction of gas has turned into stars) increases in direct proportion to Σ (equation 1; see references in Introduction). Essentially, the strength of gravity scales $\propto G\,M^2/R^2 \propto M\,\Sigma$, while the strength of feedback is proportional to the number of massive stars $\propto M$. So SF becomes more efficient, until the gas depletion time-scale becomes comparable to the free-fall time, and the gas is exhausted before it can collapse to yet higher densities (even if it is getting denser as rapidly as possible, by collapsing at the escape velocity). Adopting standard scalings for the efficiency of feedback from simulations of star-forming clouds that span the relevant range of densities (Paper II), we show this predicts a $\Sigma_{\rm max}$ in good agreement with that observed.

This explanation has several advantages over the previously proposed explanations of the maximum surface density from Paper I. As Paper II found that the parameters $\epsilon_{\rm ff}^{\rm max}$ and $\Sigma_{\rm crit}$ were insensitive to spatial scale below ∼1 kpc, our explanation applies equally well across the *entire* range of sizes of observed stellar systems in Fig. 1. Paper II also found SFE to be relatively insensitive to metallicity, so the $\Sigma_{\rm max}$ we calculate is not specific to a particular metallicity. The main effect of metallicity is the aforementioned opacity to re-processed FIR emission, but radiation hydrodynamics simulations of SF in the IR-thick limit (Skinner & Ostriker 2015; Tsang & Milosavljević 2018) have shown that this can only reduce $\varepsilon_{\rm ff}$ by ∼30 per cent, down to levels consistent with Paper II. At fixed Σ, this explanation is also insensitive to the three-dimensional density, N-body relaxation time, formation redshift, and escape velocity of the stellar systems (see e.g. fig. 4 in Paper II).

This model also explains why SF in a pre-existing dense stellar system does not generally drive Σ_* beyond $\Sigma_{\rm max}$ – in other words, if one continuously or repeatedly 'trickled' gas into e.g. a galaxy centre, why could not one continuously add new stars to the central cusp, eventually exceeding $\Sigma_{\rm max}$? The key here is that the pre-existing stellar mass still contributes to the binding force of gravity: recall, Σ in our model is the *total* mass, of gas + stars. This drives up the SFE whenever the *total* surface density exceeds $\Sigma_{\rm crit}$. Thus, for example, if fresh gas falls coherently into the centre of a bulge or dwarf nucleus with $\Sigma \sim \Sigma_{\rm max}$, then the total surface density will exceed $\Sigma_{\rm crit}$ out at larger radii, driving the SFE to high values and exhausting the gas. Multiple SF episodes would therefore be expected to build up the stellar mass by *increasing the radius inside of which* $\Sigma \sim \Sigma_{max}$, *not* by increasing $\Sigma_{\rm max}$.

We also stress, of course, that $\Sigma_{\rm max}$ is not a 'hard' limit, either in observations (Figs 1 and 2), or in our model (Fig. 4). *Some* gas can survive to reach higher densities (and must, to fuel supermassive black holes, for example), and some gas may be re-injected by stellar mass loss in these dense nuclei. And the key parameters of our model (the efficiency of feedback, which appears in $\Sigma_{\rm crit}$, and $\epsilon_{\rm ff}^{\rm max}$) are not expected to be *precisely* universal, as e.g. variations in IMF sampling (since massive stars dominate the feedback) will alter $\Sigma_{\rm crit}$ and the exact geometry of collapse will alter $\epsilon_{\rm ff}^{\rm max}$ (at the tens of per cent level).

[4]Indeed, there is at least one YMC in M83 with central surface density in excess of $10^6 M_\odot\,{\rm pc}^{-2}$ in the catalogue of Ryon et al. (2015), suggesting that the same bound for *central* surface density might not strictly hold.

ACKNOWLEDGEMENTS

We thank Arjen van der Wel for providing the galaxy size and mass data from van der Wel et al. (2014). Support for MG and PFH was provided by an Alfred P. Sloan Research Fellowship, NASA ATP Grant NNX14AH35G, and NSF Collaborative Research grant number 1411920 and CAREER grant number 1455342. Numerical calculations were run on the Caltech compute clusters 'Zwicky' (NSF MRI award number PHY-0960291) and 'Wheeler'.

REFERENCES

Bastian N., Saglia R. P., Goudfrooij P., Kissler-Patig M., Maraston C., Schweizer F., Zoccali M., 2006, A&A, 448, 881
Bastian N., Schweizer F., Goudfrooij P., Larsen S. S., Kissler-Patig M., 2013, MNRAS, 431, 1252
Bolatto A. D., Leroy A. K., Rosolowsky E., Walter F., Blitz L., 2008, ApJ, 686, 948
Bonnell I. A., Bate M. R., Vine S. G., 2003, MNRAS, 343, 413

Böker T., Sarzi M., McLaughlin D. E., van der Marel R. P., Rix H.-W., Ho L. C., Shields J. C., 2004, AJ, 127, 105
Dekel A., Krumholz M. R., 2013, MNRAS, 432, 455
Evstigneeva E. A., Gregg M. D., Drinkwater M. J., Hilker M., 2007, AJ, 133, 1722
Fall S. M., Krumholz M. R., Matzner C. D., 2010, ApJ, 710, L142
Faucher-Giguère C.-A., Quataert E., Hopkins P. F., 2013, MNRAS, 433, 1970
Federrath C., 2015, MNRAS, 450, 4035
Federrath C., Klessen R. S., 2012, ApJ, 761, 156
Geha M., Guhathakurta P., van der Marel R. P., 2002, AJ, 124, 3073
Grudić M. Y., Guszejnov D., Hopkins P. F., Lamberts A., Boylan-Kolchin M., Murray N., Schmitz D., 2018b, MNRAS, 481, 688
Grudić M. Y., Hopkins P. F., Faucher-Giguère C.-A., Quataert E., Murray N., Kereš D., 2018a, MNRAS, 475, 3511(Paper II)
Guszejnov D., Hopkins P. F., Grudić M. Y., Krumholz M. R., Federrath C., 2018, MNRAS, 480, 182
Hopkins P. F., 2012, MNRAS, 423, 2016
Hopkins P. F., Keres D., Onorbe J., Faucher-Giguere C.-A., Quataert E., Murray N., Bullock J. S., 2014, MNRAS, 445, 581
Hopkins P. F., Murray N., Quataert E., Thompson T. A., 2010, MNRAS, 401, L19(Paper I)
Hopkins P. F., Quataert E., Murray N., 2012, MNRAS, 421, 3488
Kennicutt R. C., Evans N. J., 2012, ARA&A, 50, 531
Kennicutt R. C., Jr., 1998, ApJ, 498, 541
Keto E., Ho L. C., Lo K.-Y., 2005, ApJ, 635, 1062
Kim J.-h. et al., 2018, MNRAS, 474, 4232
Klessen R. S., Burkert A., 2001, ApJ, 549, 386
Kormendy J., Fisher D. B., Cornell M. E., Bender R., 2009, ApJS, 182, 216
Krumholz M. R., Dekel A., McKee C. F., 2012, ApJ, 745, 69
Krumholz M. R. et al., 2014, Beuther H., Klessen R. S., Dullemond C. P., Henning Th., eds, Protostars and Planets VI, University of Arizona Press, Tucson, AZ, p. 243
Larson R. B., 1981, MNRAS, 194, 809
Lauer T. R. et al., 2007, ApJ, 664, 226
Lu J. R., Ghez A. M., Hornstein S. D., Morris M. R., Becklin E. E., Matthews K., 2009, ApJ, 690, 1463
McCrady N., Graham J. R., 2007, ApJ, 663, 844
Murray N., Quataert E., Thompson T. A., 2010, ApJ, 709, 191
Norris M. A. et al., 2014, MNRAS, 443, 1151
Orr M. E. et al., 2018, MNRAS, 478, 3653
Ostriker E. C., Shetty R., 2011, ApJ, 731, 41
Portegies Zwart S. F., McMillan S. L. W., Gieles M., 2010, ARA&A, 48, 431
Raskutti S., Ostriker E. C., Skinner M. A., 2016, ApJ, 829, 130
Rejkuba M., Dubath P., Minniti D., Meylan G., 2007, A&A, 469, 147
Ryon J. E. et al., 2015, MNRAS, 452, 525
Schweizer F., Seitzer P., 2007, AJ, 133, 2132
Skinner M. A., Ostriker E. C., 2015, ApJ, 809, 187
Thompson T. A., Krumholz M. R., 2016, MNRAS, 455, 334
Thompson T. A., Quataert E., Murray N., 2005, ApJ, 630, 167
Tsang B. T. H., Milosavljević M., 2018, MNRAS, 478, 4142
van der Wel A. et al., 2014, ApJ, 788, 28

This paper has been typeset from a TEX/LATEX file prepared by the author.